Journal of Crystal Growth 323 (2011) 76–79

Contents lists available at ScienceDirect

Journal of Crystal Growth

journal homepage: www.elsevier.com/locate/jcrysgro

Growth of non-polar GaN on $LiGaO_2$ by plasma-assisted MBE

R. Schuber [a,b], Y.L. Chen [c], C.H. Shih [c], T.H. Huang [d], P. Vincze [e], I. Lo [e], L.W. Chang [d], Th. Schimmel [a,e], M.M.C. Chou [c], D.M. Schaadt [a,b,*]

[a] Institute for Applied Physics, Karlsruhe Institute of Technology (KIT), 76131 Karlsruhe, Germany
[b] DFG-Center for Functional Nanostructures (CFN), Karlsruhe Institute of Technology (KIT), 76131 Karlsruhe, Germany
[c] Department of Physics, National Sun Yat-Sen University, Kaohsiung 80424, Taiwan, ROC
[d] Department of Materials Science and Opto-electronic Engineering, National Sun Yat-Sen University, Kaohsiung 80424, Taiwan, ROC
[e] Institute of Nanotechnology, Karlsruhe Institute of Technology (KIT), 76131 Karlsruhe, Germany

ARTICLE INFO

Available online 27 October 2010

Keywords:
B1. Non-polar nitrides
B1. $LiGaO_2$
B1. GaN
A3. Molecular beam epitaxy

ABSTRACT

We show that non-polar *M*-plane and *A*-plane GaN can be grown on $LiGaO_2$ with very high phase purity. The morphology of the GaN surfaces is influenced by the underlying substrate morphology, which exhibits a high abundance of surface scratches. Nevertheless, the root-mean-square roughness of the samples is low, i.e. 2.9 nm for *M*-plane GaN and 10 nm for *A*-plane GaN. The predominant defects in the GaN films are threading dislocations and stacking faults.

1. Introduction

Due to a large number of beneficial material properties, group III-nitrides have had an enormous influence on compound semiconductor research over the past years. Nevertheless, improvements and developments in the crystal quality and orientation are still underway. One important issue is that group III-nitrides grown along the $\langle 0\,0\,0\,1 \rangle$ direction show a strong quantum confined Stark effect due to the electric fields resulting from the spontaneous and piezoelectric polarization. These fields cause a reduced oscillator strength due to a spatial separation of electrons and holes and a decrease in the energy of the radiative transition. This situation can be avoided considering the hexagonal structure of group III-nitrides.

Epitaxial layers with non-polar surfaces such as the *M*-plane $\{1\,\bar{1}\,0\,0\}$ and *A*-plane $\{1\,1\,\bar{2}\,0\}$ are attractive due to the absence of built-in electrical fields in growth direction. It has been shown that multiple quantum well structures on the basis of *M*-plane GaN indeed exhibit higher quantum efficiency and a shift towards shorter wavelengths, compared to *C*-plane structures, as a consequence of the lacking internal electrostatic fields [1].

Since non-polar GaN substrates are not readily available for homoepitaxy, various alternative substrates have been examined for growth of high quality non-polar GaN crystals. In this sense β- $LiGaO_2$ (LGO) presents a very closely lattice matched substrate for GaN heteroepitaxy. The LGO crystal can be grown by the Czochralski method and is thermally stable up to about 1600 °C [5]. Further, it can be selectively etched with respect to nitrides. While growth of *C*-plane GaN on (0 0 1) LGO has already been investigated in the past by a number of groups, e.g. [2], we now have examined the growth of non-polar *M*-plane GaN on (1 0 0) LGO [3] and *A*-plane GaN on (0 1 0) LGO [4]. Here we will show a comparison of both these non-polar GaN films on LGO.

A big advantage of LGO over $LiAlO_2$ (LAO), a chemically similar crystal often used for *M*-plane GaN growth, is the growth of specific GaN planes on different LGO planes, which automatically lead to a high phase purity of the GaN film. While both *C*- and *M*-plane GaN are reasonably lattice matched to (1 0 0) LAO, the lattice and underlying crystal symmetry is only matched well for *M*-plane GaN on (1 0 0) LGO, *A*-plane GaN on (0 1 0) LGO and *C*-plane GaN on (0 0 1) LGO. Fig. 1 displays the (1 0 0) LGO and (0 1 0) LGO surface with possible nucleation sites of *M*-plane and *A*-plane GaN, respectively.

2. Experimental procedure

The (1 0 0) and (0 1 0) LGO substrates were grown at the National Sun Yat-sen University in Taiwan and polished by a commercial vendor. The GaN samples were grown in a RIBER Compact 21 MBE system dedicated to the growth of nitrides. Due to transparency of the substrate in the visible and near infrared wavelength range the substrate was mounted onto a Si wafer using a thin layer of In to provide a homogeneous thermal coupling. The substrates were inserted into molybdenum holders and first outgased for 60 min at 130 °C in a load lock chamber before transferring them into the growth chamber. Activated nitrogen was supplied by an Oxford HD25 RF plasma cell operated at a gas

* Corresponding author at: DFG-Center for Functional Nanostructures (CFN), Karlsruhe Institute of Technology (KIT), 76131 Karlsruhe, Germany.
E-mail address: daniel.schaadt@kit.edu (D.M. Schaadt).

0022-0248/$ - see front matter © 2010 Elsevier B.V. All rights reserved.
doi:10.1016/j.jcrysgro.2010.10.118

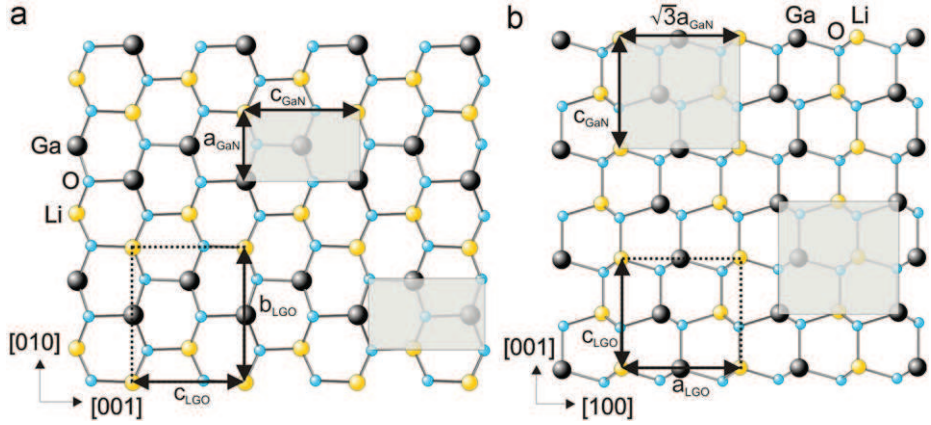

Fig. 1. Ball and stick model of the (1 0 0) LGO (a) and the (0 1 0) LGO (b) surface. The dotted rectangles signal the size of the LGO unit cell, while the shaded rectangles with continuous lines indicate possible nucleation sites for (1 $\bar{1}$ 0 0) and (1 1 $\bar{2}$ 0) GaN, respectively.

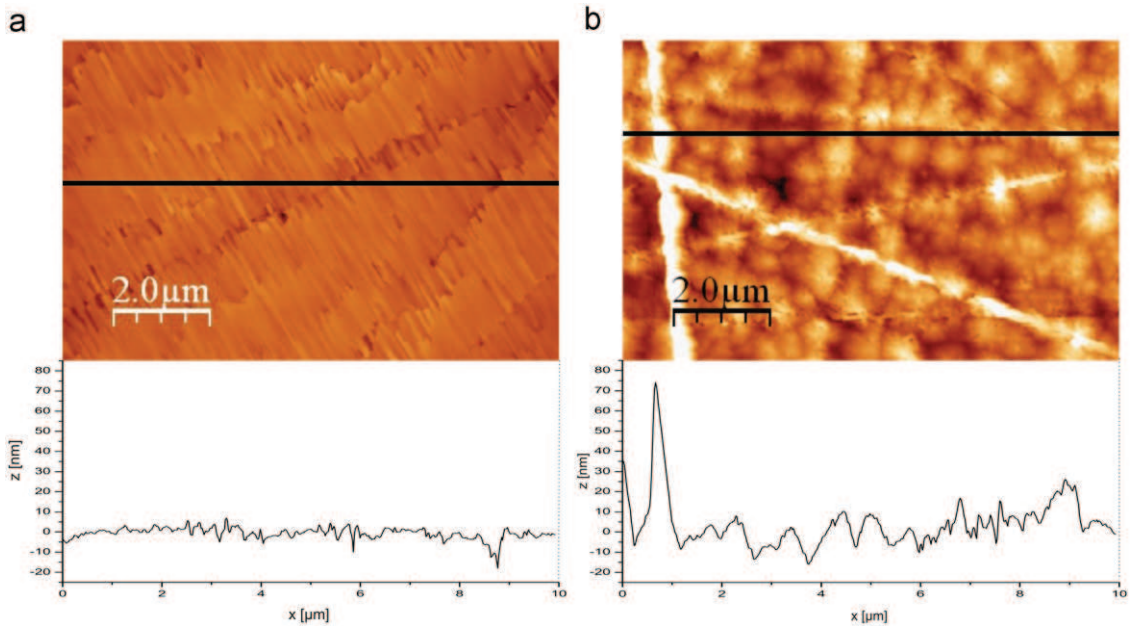

Fig. 2. AFM images of the *M*-plane (a) and the *A*-plane (b) GaN surface. Beneath the images a line profile, taken along the horizontal line indicated in the image above, is given for each image, respectively.

flow of 0.3 sccm and 450 W forward power. A growth rate of roughly 100 nm/h for the *M*-plane GaN film and 50 nm/h for the *A*-plane GaN film was used. This resulted in film thicknesses of approximately 390 nm and 170 nm for the *M*- and *A*-plane GaN films as measured by scanning electron microscopy, respectively.

A challenge concerning GaN growth on LGO is the tendency of the epitaxial films to peel off of the substrate. This lifting-off of the epitaxial film from the substrate may be caused by damage to the substrate surface as a consequence of the irradiation of the substrate with the electron beam from *in situ* reflective high energy electron diffraction (RHEED) measurements. Another reason could be the strain induced into the film by the unequal anisotropic coefficients of thermal expansion (CTE) between LGO and GaN in the temperature range between room and growth temperature (700 °C) [3]. We found that keeping the exposure time of the sample to the RHEED beam to a minimum and annealing of the substrates to be important steps to ensure film stability, i.e. to prevent a peeling off of the substrate. In contrast, substrate cleaning via Ga desorption or exposing the LGO substrate to activated nitrogen at elevated temperatures has no or deteriorating influences on the epitaxial film stability.

Growth was monitored *in situ* using RHEED. Atomic force microscopy (AFM) was used to reveal the morphology of the GaN films. X-ray diffraction (XRD) gives information about the phase purity and strain state of the films. Samples for cross sectional and plan view transmission electron microscopy (TEM) were prepared by focussed ion beam and mechanical polishing.

3. Results and conclusion

Although the bulk crystal quality of the substrate, LGO, is very high as determined from X-ray rocking curves (FWHM of (2 0 0) LGO and (0 4 0) LGO are 23 and 18 arcsec, respectively), the polishing of epi-ready substrates needs improvement. AFM images (not shown here) reveal a large number of surface scratches with root-mean-square (rms) roughness values on the order of 10–20 nm over an area of $10 \times 10 \mu m^2$. These surface scratches originating from the substrate are also seen in AFM images of the surfaces of the GaN epitaxial layers seen in Fig. 2. The rms value for the *M*-plane GaN surface over $10 \times 10\ \mu m^2$ was measured to be as low as 2.9 nm. The *A*-plane GaN surface shows a higher rms value

which amounts to about 10 nm in an area of $8 \times 8\ \mu m^2$, where an area was considered omitting the most pronounced scratches.

In situ RHEED measurements indicate a smooth film surface by showing streaky diffraction patterns. First evidence of the crystal orientation of the GaN film can be gained by comparing the ratio of the line separation in [0 0 0 1] direction and the direction perpendicular to it, i.e. the [1 1 $\bar{2}$ 0] and [1 $\bar{1}$ 0 0] direction for *M*-plane and *A*-plane GaN, respectively. Fig. 3(a) and (b) show the two diffraction patterns separated by 90° of the *M*-plane GaN sample while the equivalent RHEED patterns of the *A*-plane GaN sample can be seen in Fig. 3(c) and (d).

Fig. 4 depicts results obtained by x-ray diffraction measurements on the two samples. Fig. 4(a) shows two sections of an ω–2θ scan on the *M*-plane GaN film. Part (b) of the same figure shows two regions of the scan of the *A*-plane GaN sample. In both cases the high phase purity of at least 99% is apparent, i.e. a *C*-plane GaN component in any of the two films is lower than 1%. From the relative shift of the GaN peaks to the substrate peak, which is assumed to be completely relaxed, the strain state of the films is estimated. The 390 nm thick *M*-plane GaN film is relaxed to roughly 80% compared to the maximal possible transverse deformation caused by the lattice mismatch between the substrate and the GaN film. For the 170 nm thick *A*-plane GaN film a relaxation state of approximately 50% was found.

TEM analysis of the GaN films confirms the epitaxial relationship, i.e. [1 1 $\bar{2}$ 0] GaN ∥[0 1 0] LGO and [0 0 0 1] GaN∥ [0 0 1] LGO for *M*-plane GaN as well as [1 $\bar{1}$ 0 0] GaN ∥[1 0 0] LGO and [0 0 0 1] GaN∥ [0 0 1] LGO for *A*-plane GaN. Further, threading dislocations and stacking faults are seen to be the major defects present in both films. Fig. 5(a) and (b) shows bright field images of the *M*- and *A*-plane GaN cross sectional TEM samples, respectively, with the plane of the cross section perpendicular to the [0 0 0 1] direction. The high density of threading dislocations is apparent. In these images stacking faults are not visible, as they lie in the *C*-plane. However, inversion domain

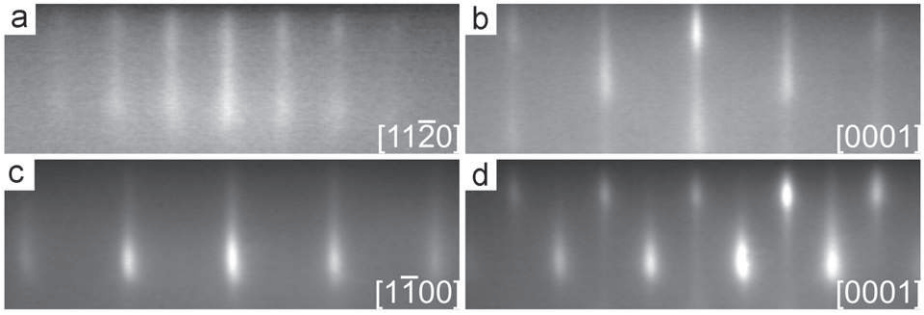

Fig. 3. (a and b) RHEED images of the *M*-plane GaN azimuths, separated by 90°. The spacing of the streaks in [1 1 $\bar{2}$ 0] direction gives the c_{GaN} lattice constant whereas the a_{GaN} lattice constant is given by the separation of streaks in [0 0 0 1] direction. (c and d): RHEED patterns of two perpendicular *A*-plane GaN azimuths. Here the spacing of the streaks in [1 $\bar{1}$ 0 0] direction correspond to $\sqrt{3}a_{GaN}$.

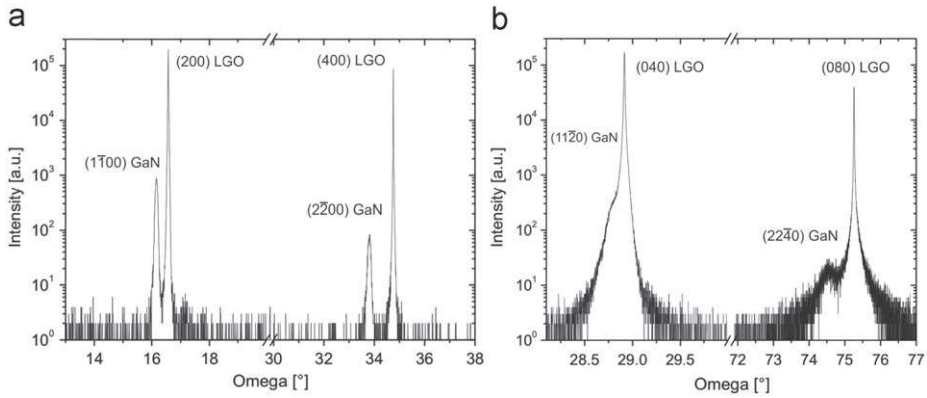

Fig. 4. Two ω–2θ X-ray scans in double crystal configuration of GaN layers grown on LGO are shown in the graphs: (a) shows two sections of the measurement of the *M*-plane GaN sample while (b) shows the result obtained measuring the *A*-plane GaN sample.

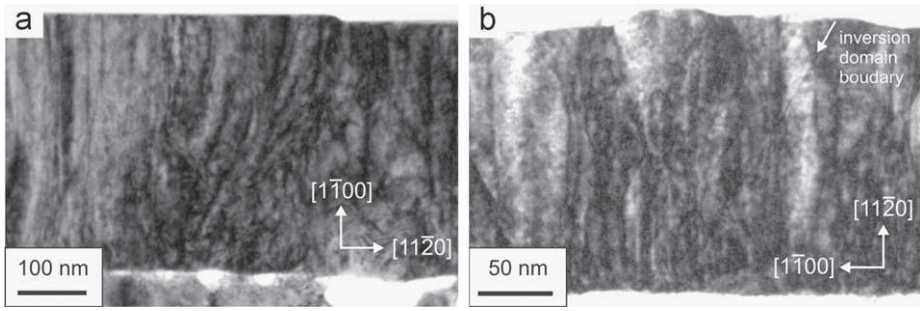

Fig. 5. Bright field images taken of the cross sectional TEM samples of the *M*-plane (a) and *A*-plane (b) GaN sample. In both images the observer is looking into the [0 0 0 1] direction. In each case the substrate is located at the bottom of the picture. The (a) sample was cut by FIB, the sample seen in (b) was fabricated by mechnical polishing.

boundaries, confining stacking faults, are visible in Fig. 5(b) as straight lines running across the image at an angle of 60°. The plan view TEM sample of the *M*-plane GaN film allows calculation of the density of threading dislocations and stacking faults which lie in the order of 1×10^{11} cm^{-2} and 2×10^{5} cm^{-1}, respectively. Judging from the cross sectional TEM data for the *A*-plane GaN sample a similar value for the density of threading dislocations is expected. However, less stacking faults are present in the *A*-plane GaN film. This can be seen in the cross sectional TEM image cut perpendicular to the [1 $\bar{1}$ 0 0] direction (not shown here). A confirmation of this observation is given by the fact that lines elongated from the diffraction spots in c direction, indicating the presence of stacking faults, are present in the diffraction pattern of the *M*-plane GaN TEM sample (cut perpendicular to the [1 1 $\bar{2}$ 0] direction) but are missing in the *A*-plane GaN sample (cut perpendicular to the [1 $\bar{1}$ 0 0] direction).

4. Summary

Our results prove experimentally the expected epitaxial relationship of *M*-plane GaN on (1 0 0) LGO and *A*-plane GaN on (0 1 0) LGO. From the data collected we find a high phase purity of the grown GaN films. Surface scratches present in the GaN films origin from scratches in the substrate. We expect to obtain smoother surfaces and a higher crystal quality of the GaN films when mechanical polishing of the substrate as well as growth conditions have been optimized. The main defects in the GaN films are threading dislocations and stacking faults.

Acknowledgements

The authors from Karlsruhe acknowledge financial support from the Deutsche Forschungsgemeinschaft (DFG) and the State of Baden-Württemberg through the DFG-Center for Functional Nanostructures (CFN) within the sub project A 2.7 and A 4.6. One of the authors (R. Schuber) is grateful for support from the Karlsruhe House of Young Scientists (KHYS) for providing a research scholarship which helped contribute to this work.

References

[1] P. Waltereit, O. Brandt, A. Trampert, H.T. Grahn, J. Menniger, M. Ramsteiner, M. Reiche, K.H. Ploog, Nature 406 (2000) 865–868.
[2] W.A. Doolittle, S. Kang, T.J. Kropewnicki, S. Stock, P.A. Kohl, A.S. Brown, J. Electron. Mater. 27 (1998) L58–L60.
[3] R. Schuber, M.M.C. Chou, D.M. Schaadt, Thin Solid Films 518 (2010) 6773–6776.
[4] R. Schuber, M.M.C. Chou, P. Vincze, Th. Schimmel, D.M. Schaadt, J. Cryst. Growth 312 (2010) 1665–1669.
[5] S. Weise, H. Neumann, Cryst. Res. Technol. 31 (1996) 659–664.